Quantum Electronics **46** (5) 432–436 (2016)

DOI: 10.1070/QEL16032

Acceleration of multiply charged ions by a high-contrast femtosecond laser pulse of relativistic intensity from the front surface of a solid target

S.A. Shulyapov, I.M. Mordvintsev, K.A. Ivanov, P.V. Volkov,
P.I. Zarubin, I. Ambrožová, K. Turek, A.B. Savel'ev

Abstract. **It is shown that the acceleration efficiency of protons and multiply charged ions (and also the charge composition of the latter) accelerated backwards under irradiation of the front surface of thick solid targets by high-power femtosecond laser radiation with an intensity of 2×10^{18} W cm^{-2} is determined by the contrast of this radiation. Thus, highly ionised ions up to C^{6+}, Si^{12+} and Mo^{14+} are recorded on polyethylene, silicon and molybdenum targets at a contrast of 10^{-8}, the ions with charges up to C^{5+}, Si^{10+} and Mo^{10+} possessing an energy of more than 100 keV per unit charge. In the case of a metal target, the acceleration efficiency of protons is significantly reduced, which indicates cleaning of the target surface by a pre-pulse. The measurements performed at a contrast increased by two-to-three orders of magnitude show the presence of fast protons (up to 300–700 keV) on all targets, and also a decrease in the energy and maximum charge of multiply charged ions.**

Keywords: *relativistic intensity, contrast, laser plasma, ion acceleration, multiply charged ions, collision ionisation.*

1. Introduction

One of the urgent problems in interaction of intense laser radiation with matter is the development of an effective source of multiply charged ions [1–3]. The studies in this area not only are of fundamental importance, but also open wide opportunities for practical application of such a source [4–6].

Generation of multiply charged ions is commonly performed using high-power sub-petawatt laser systems with a pulse intensity of more than 5×10^{19} W cm^{-2} [2, 7]. This is conditioned by the need to use high-intensity laser fields for deep ionisation of atoms in a target and a high pulse energy for producing a high-intensity flux of accelerated particles. Furthermore, a thin organic layer containing protons is commonly present at the target surface, acceleration of which impedes the power transfer to heavier ions. This effect can be eliminated by cleaning of the target surface immediately prior to the irradiation by a laser pulse [8–10].

This paper is devoted to investigating the role of the laser pulse contrast and clarifying the mechanisms of deep ionisation of target atoms. Understanding of these processes is crucially important for the experiments on acceleration of charged ions. It appears that for these studies it is reasonable to use desktop laser systems of terawatt peak power, which allow generating pulses of relativistic intensity and, at the same time, are much more convenient in comparison with petawatt complexes to carry out experiments in the case of a wide variation of experimental configurations. In particular, the pulse repetition rate in such systems is large; the systems possess small sizes, etc. The optimal experimental configurations determined by means of compact laser systems (pre-pulse parameters, target characteristics) can be further used in the experiments with high (ultimate) intensities. Moreover, the obtained characterisitcs of laser-plasma interactions can be reproduced by using more powerful laser systems at not so high intensities typical of the studies we have conducted (for example, in order to increase the particle flow). This is essential for practical applications in which the charge and number of ions, but not their maximal energy, are of importance.

2. Experimental setup

The experimental setup is shown in Fig. 1. The studies have been performed using radiation from a Ti:sapphire laser system at the International Laser Centre, M.V. Lomonosov Moscow State University (ILC MSU). The laser beam with a wavelength of 800 nm is p-polarised, the pulse repetition rate is 10 Hz, the pulse duration is 45 ± 5 fs, the pulse energy is 10 mJ and the peak intensity is estimated as 2×10^{18} W cm^{-2}.

The temporal profile of the laser pulse contains a nanosecond pre-pulse (–14 ns) with the contrast of 5×10^{-8}, the level of amplified spontaneous emission (ASE) is $\sim10^{-8}$ (from –175 to –10 ps) and picosecond pre-pulses are absent. It should be noted that, at the intensities close to the plasma formation threshold [11], the ASE and pre-pulse may form a low-density pre-plasma layer on the target surface, preserving the vacuum–plasma boundary rather sharp. The laser pulse contrast can be improved by introducing into the scheme a crystal to generate a crossed-polarised wave (XPW) [12], with the ASE level falling below 10^{-10}.

The radiation is focused on the target using an off-axis parabolic mirror ($F\approx75$ mm, $F/D\approx5$) at an angle of 45° to its surface. The plates of molybdenum (Mo) and silicon (Si) with a thickness of 2 and 0.5 mm, respectively, are used as

S.A. Shulyapov, I.M. Mordvintsev, K.A. Ivanov, R.V. Volkov, A.B. Savel'ev Department of Physics and International Laser Centre, M.V. Lomonosov Moscow State University, Vorob'evy Gory, 119991 Moscow; e-mail: ser270489@yandex.ru;
P.I. Zarubin Joint Institute for Nuclear Research, ul. Zholio-Kyuri 6, 141980 Dubna, Moscow region, Russia;
I. Ambrožová, K. Turek Department of Radiation Dosimetry, Nuclear Physics Institute of the Czech Academy of Sciences, Na Truhlářce 39/64, CZ-180 86 Prague 8, Czech Republic

Received 18 February 2016; revision received 11 April 2016
Kvantovaya Elektronika **46** (5) 432–436 (2016)
Translated by M.A. Monastyrskiy

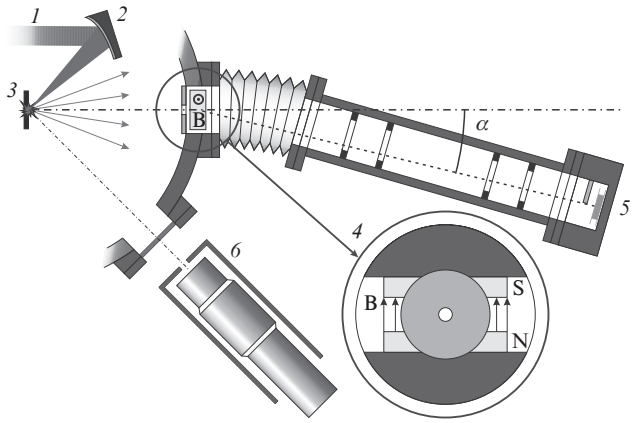

Figure 1. Schematic of the experimental setup: (*1*) laser radiation; (*2*) parabolic mirror; (*3*) target; (*4*) aperture and magnet; (*5*) microchannel plate (MCP); (*6*) detector of γ-radiation.

targets; a polyethylene (CH_2) film with a thickness of 100 μm is glued to the surface of some Mo plates. All the experiments have been performed in a vacuum chamber with a residual pressure better than 4×10^{-5} Torr.

Ions are recorded by means of a VEU-7M-4 time-of-flight magnetic spectrometer detector based on a chevron microchannel plate (MCP). The spectrometer's entrance is located on the normal to the target. The magnetic field B is generated by two neodymium magnets with the size of 4×8×30 mm, separated by 8 mm, and reaches 0.207 T on the central axis between them. A collimating aperture (D_{ap} = 1 or 2 mm) is placed in front of the magnets. The distance from the plasma to magnets constitutes 26 cm, from the magnets to MCP – 129 cm. The presence of a bellow unit located between the magnet and MCP allows varying the angular position (α) of the MCP with respect to the diaphragm axis. The deflection angle of ions in the magnet is $\alpha_i \propto (1/v)(Z/m)$, where v, Z and m are velocity, charge and mass of the ion, respectively. Thus, by measuring the temporal signal from the MCP at a fixed $\alpha = \alpha_i$, the ions entering the detector can be classified by the charge-to-mass ratio Z/m and their characteristics can be calculated. As an example, Fig. 2 shows a temporal signal from the MCP, averaged over ~800 realisations (the so-called ion current) obtained on a CH_2 target at $\alpha \approx 2.6°$. In addition to the spectrometer described above, a tracking detector (the CR39 plates [13]) has been used for proton recording.

The laser pulse quality was monitored by measuring the integral output of the γ-radiation of plasma by using a scintillation detector based on a photomultiplier tube and a 63-mm-thick NaI(Tl) crystal.

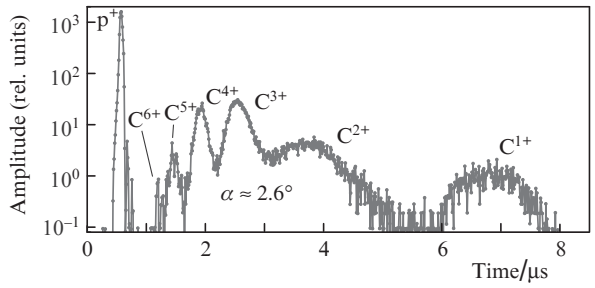

Figure 2. Averaged temporal signal from the MCP for a CH_2 target.

By employing the results of measuring the γ-radiation spectrum of plasma for a Mo target, evaluation of the average energy of hot electrons was conducted (the technique is described in [14]). Two hot electronic components with the 'temperatures' of ~30 keV and 185 ± 10 keV are present in plasma. Hereinafter, the temperature of electrons or ions is regarded as a parameter T responsible for the attenuation rate in a relevant energy spectrum approximated by an exponential function of the form $N(E) \propto \exp(-E/T)$ [15, 16]. The processes of resonant absorption [15, 17] and/or ponderomotive acceleration [18] are responsible for generating the hottest electronic component.

3. Cleaning of the metal target surface

As a result of our studies, it is found that the proton acceleration efficiency at a contrast of 10^{-8} is small. This is most clearly manifested in the case of a metal (Mo) target. As previously mentioned, a thin layer of hydrocarbon compounds, oxides and water located on the target surface contains protons. At $Z/m = 1$, those protons are efficiently accelerated in laser plasma and typically represent the most intense of ionic components [1, 8, 19] (see Fig. 2).

At the same time, our measurements have shown that, at the contrast of ~10^{-8} in the case of the Mo target, the maximum energy of protons only constitutes 81 ± 5 keV [Fig. 3, curve (*2*)], whereas it reaches 340 ± 40 and 740 ± 170 keV in the case of Si and CH_2 targets, respectively [Fig. 3, curves (*3*) and (*4*)]. The spectra for all three types of the targets contain a proton component with a temperature of ~30 keV (Mo – 25 ± 2 keV, Si – 34 ± 1 keV and CH_2 – 33 ± 4 keV). Note that a similar temperature is peculiar to a less energetic component of the two hot electronic ones generated by plasma. One more proton component with a higher temperature of 94 ± 11 keV is observed in the spectrum on the CH_2 target, which may be associated with the presence of hydrogen atoms in the target, and also with its low conductivity [20].

In the case of the Mo target, the CR39 plates [13] located close to the target (9.5 cm) were additionally used to increase the measurement sensitivity in proton recording. Some of the plates were covered by a filter in the form of a 1-μm-thick lavsan film. After the exposure (about 200 shots), the plates

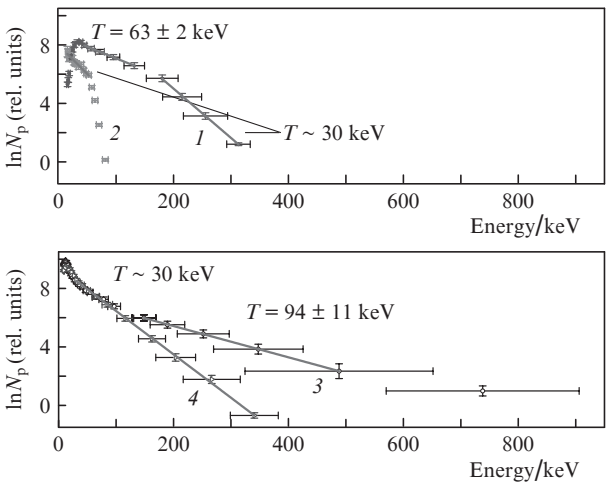

Figure 3. Energy spectrum of protons on the Mo target at an elevated laser pulse contrast (*1*), and also on Mo (*2*), CH_2 (*3*) and Si (*4*) targets at normal contrast.

were etched for two hours in 30% KOH solution to make ion tracks visible. Figure 4 shows enlarged photographs of the plates' front surfaces. It is seen that, after passing the filter, the flux of protons is greatly reduced – from more than 4×10^6 to 10^4 particles per steradian per shot. A simulation using the SRIM package [21] has shown that the H, C, O and Mo ions should have the energy of ~90, 350, 450 and 1700 keV, respectively, in order to pass through a 1-μm-thick lavsan film. Thus, the maximum energy of protons constitutes ~90 keV, which coincides with the result obtained by means of a spectrometer.

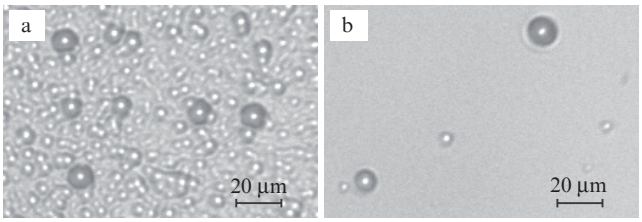

Figure 4. Enlarged photographs of the front surfaces of CR39 plates in experiments with the Mo target – (a) uncovered and (b) covered by a lavsan film of 1 μm thickness. Small funnels correspond to proton tracks, large funnels – to the tracks of heavier ions (C, O, Mo).

Such a low energy of fast protons can be explained by ablation or evaporation of the target surface layer by the action of a pre-pulse (or ASE) with the formation of a preplasma low-density gradient, in which the ions are accelerated less efficiently than on the sharp target edge [10]. The plasma formation threshold for metals is several times lower than that for dielectrics [11], and so cleaning of the Mo-target surface is much more efficient than in the case of Si and CH_2 targets.

The conclusions confirm the experiments with Mo and Si targets at the increased laser radiation contrast. When using the XPW in the case of the Mo target, two components of fast protons with the temperatures of 30±1 and 63±2 keV are observed in the energy spectrum, their maximum energy being increased up to 310±20 keV [Fig. 3, curve (*1*)]. On the Si target, the maximum energy and the temperature of fast protons also increase, but not so significantly, and constitute 550±50 and 42±4 keV, respectively.

Note that the laser pre-pulse has previously been used in the works of both our laboratory [9, 10] and other authors [22, 23] to clean the target surface at moderate laser intensities. The distinctive feature of this work is a demonstration of the effect of self-cleaning of the target without the use of any special pre-pulses at a relativistic intensity of laser radiation.

4. Generation of multiply charged ions

A key result of the conducted experiments, which is observable for all the targets used, is the recording of ions with a high ionisation multiplicity (up to C^{6+}, Si^{12+} and Mo^{14+}).

The ions with a low ionisation multiplicity (up to C^{4+}, Si^{7+} and Mo^{6+} inclusive) have approximately the same maximum energies E_{max} per unit charge Z, amounting to 250–300 keV, i.e. $E_{max} \propto ZT_{he}$ [16], where T_{he} = 185 keV is the temperature of the most hot electron component, and the proportionality coefficient equals to 1.6±0.1. With a further charge increase, the ratio E_{max}/Z decreases and, in the case of C^{6+}, Si^{12+} and Mo^{14+} ions, constitutes 82±5, 41±3 and 45±4 keV, respectively. Note that the maximum energies of Mo^{7+} – Mo^{9+} ions have not been determined in the measurements due to insufficient smallness of the step with respect to α (see Fig. 1), and therefore it is impossible to claim with certainty that reduction of the ratio E_{max}/Z for Mo ions starts when the ionisation multiplicity exceeds 6+.

Experiments carried out on the Mo and Si target at an elevated laser pulse contrast show that in this case the ratio E_{max}/Z for multiply charged ions turns out 2–5 times lower than without using the XPW. In addition, the Si^{11+} and Si^{12+} ions stop to be observed on Si targets, i.e. the maximum ionisation multiplicity is reduced.

Consider possible mechanisms of emergence of the multiply charged C, Si and Mo ions. The collisional ionisation [24, 25] plays a main role in the plasma formation process; however, the atoms near the target surface can be directly ionised by the laser pulse field [26, 27], whereas the fast ions are additionally ionised by the charge separation field (ambipolar field) [28]. As the plasma cools at the expense of expansion and outflow of heat into the target, ionisation is replaced by recombination, which reduces the ion charge values [29]. A decrease in the multiplicities of ionisation is limited by the effect of their freezing, i.e. significant reduction in the recombination rate of the low-density plasma [30]. In particular, owing to this effect, the fast ions that have been pushed out to the plasma cloud's leading edge may preserve a high multiplicity of ionisation obtained in plasma.

The probability of tunnel ionisation by the field (ambipolar or laser) is exponentially dependent on the field strength and increases sharply near the critical value $E_{BSI} = \varepsilon_Z^2/(4e^3Z)$, where e is the elementary charge; ε_Z is the ionisation energy ($C^{Z-1} \to C^Z$) [26]. At the intensity $E \approx E_{BSI}$, the maximum of the atomic core's potential barrier suppressed by the field becomes equal to the energy ε_Z. The ambipolar field intensity can be estimated as $E_a \sim \sqrt{4\pi n_{he} T_{he}}$, where T_{he}, n_{he} [16], where T_{he} and n_{he} are the temperature and concentration of hot electrons. In Fig. 5, by an example of the C ions, the ionisation probability w_{amb} of a single ion by the ambipolar field (see [26, 27]) of hot electrons is shown versus their concentration at T_{he} = 185. Thus, as a result of field ionisation of the C, Si and Mo atoms at $I = 2\times10^{18}$ W cm^{-2} and $n_{he} = 10^{19}$ cm^{-3}, their ionisation multiplicity Z_{max} can reach 4+, 12+, and 16+ at ε_Z = 65, 523 and 489 eV, respectively [31].

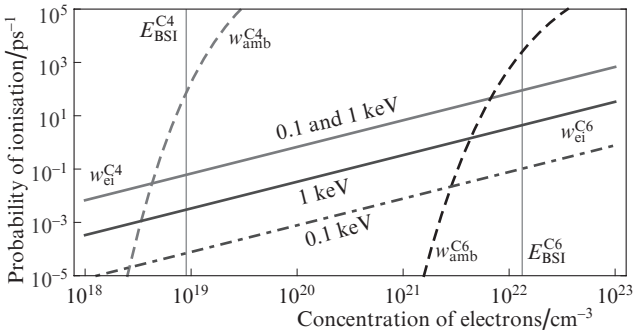

Figure 5. The probabilities (during 1 ps) of ionisation of solitary ions $C^{3+} \xrightarrow{65\,eV} C^{4+}$ (C4) and $C^{5+} \xrightarrow{490\,eV} C^{6+}$ (C6) by the ambipolar field w_{amb} and electron impact w_{ei} vs. the concentration of hot (n_{he}) and thermal (n_e) electrons, respectively. The probabilities w_{ei} are given at T_e = 0.1 keV and 1 keV (for C4 these probabilities are indistinguishable). The values of n_{he}, at which the ambipolar field of hot electrons reaches its critical value (E_{BSI}) for C4 and C6, are marked.

The laser pulse field ionises only atoms near the target surface, which are closed by a layer of organic compounds; this explains a decrease in the multiplicity of ionisation and ion energy with increasing contrast. However, a decrease in the ratio E_{max}/Z of the multiply charged ions with increasing charge (without XPW) indicates that these ions were not generated at the time of the laser pulse arrival on the target, but were additionally ionised when leaving the plasma cloud, and therefore did not gain the energy corresponding to their final charge. The fact that the C^{5+} and C^{6+} ions, which are inaccessible to field ionisation due to a high level of $E_{BSI} \propto \varepsilon_Z^2/Z$, were recorded in the experiment on a CH_2 target (see Fig. 2) also means that the ions generated by the field ionisation represent a 'seed' for further ionisation by the electron impact.

The probability w_{ei} of collisional ionisation (see [25, 32]) is not so sharply dependent on the concentration of thermal electrons ($w_{ei} \propto n_e$) as the probability of ionisation by the ambipolar field w_{amb} depends on the concentration n_{he} of hot electrons (Fig. 5), but is greatly reduced if the thermal electron temperature T_e becomes lower (or significantly higher) than the ionisation energy. In addition, the highest abundance in the equilibrium plasma have the ions, the ionisation multiplicities of which are determined by the Saha distribution [25] and correspond to $\varepsilon_Z = (2-3)T_e$ in a sufficiently dense plasma [24]. The energy ε_Z of total ionisation of the C atom constitutes 490 eV for $Z = 6+$ [31]. Initial temperature and concentration of the thermal plasma component in our conditions can be estimated as ~1 keV and 10^{21} cm^{-3} [32, 33], respectively. Assuming that fast ions (10^{10} – 10^{12} particles [32]) are strongly ionised by the field at the start of expansion, and the time of their emission from plasma constitutes 1–2 ps [16, 32], part of the highly ionised C, Si and Mo ions generated at the expense of collisional ionisation turns out considerable.

In this case, the use of thick solid-state targets in experiments plays an important role which allows one to obtain (and maintain in the course of plasma cloud expansion) the temperature and electron concentration sufficient for effective collisional ionisation, which is difficult to implement on a thin-film target.

5. Conclusions

In the course of this work, we have demonstrated the effect of cleaning of the target surface by means of a natural pre-pulse at a sufficiently high (~10^{-8}) laser radiation contrast and also a more efficient acceleration of multiply charged ions compared to the case of high contrast (less than 10^{-10}), which is associated with the cleaning effect. That effect manifests itself most strongly in the case of a metal target due to a low threshold of plasma formation. Because the problem of a required contrast level is especially urgent in the regime of ultra-relativistic intensities, this result has a great practical importance. For example, to reproduce it at the intensity of 10^{20} W cm^{-2} and pulse duration of about 50 fs, the contrast level of 2×10^{-10} is required.

Furthermore, we have shown experimentally that proton acceleration from a volume (CH_2-target) in the case of a thick target occurs more efficiently than that from a surface (Mo and Si targets).

Finally, it is commonly accepted that the maximum ionisation multiplicities of ions in femtosecond laser plasma at a high pulse intensity are attained in the process of field ionisation. Nonetheless, this paper has revealed a key role of collisional ionisation in generating the multiply charged ions using the thick solid targets. In particular, the ions C^{5+} and C^{6+} recorded in the experiment could not be obtained by means of field ionisation under the conditions described.

Acknowledgements. The work was supported by the Russian Foundation for Basic Research (Grant Nos 14-02-31871 mol_a, 13-02-00337 and 16-02-00263 A). S.A.Sh. expresses his gratitude to the RF President's Grants Council for the financial support in the form of the RF President Scholarship SP-1265.2015.2.

References

1. Daido H., Nishiuchi M., Pirozhkov A. *Rep. Prog. Phys*., **75**, 056401 (2012).
2. Nishiuchi M., Sakaki H., Maeda S., Sagisaka A., Pirozhkov A.S., Pikuz T., Faenov A., Ogura K., Kanasaki M., Matsukawa K., Kusumoto T., Tao A., Fukami T., Esirkepov T., Koga J., Kiriyama H., Okada H., Shimomura T., Tanoue M., Nakai Y., Fukuda Y., Sakai S., Tamura J., Nishio K., Sako H., Kando M., Yamauchi T., Watanabe Y., Bulanov S.V., Kondo K. *Rev. Sci. Instrum*., **85**, 02B904 (2014).
3. Shaim Md., Haider A., Elsayed-Ali Hani E. *Nucl. Instr. Meth. Phys. Res. B*, **356**, 75 (2015).
4. Ledingham K.W.D., McKenna P., Singhal R.P. *Science*, **300**, 1107 (2003).
5. Krushelnick K., Clark E.L., Allott R., Beg F.N., Danson C.N., Machacek A., Malka V., Najmudin Z., Neely D., Norreys P.A., Salvati M.R., Santala M.I.K., Tatarakis M., Watts I., Zepf M., Dangor A.E. *IEEE Trans. Plasma Sci.*, **28**, 1110 (2000).
6. Gillaspy J.D., Pomeroy J.M., Perrella A.C., Grube H. *J. Phys.: Conf. Ser*., **58**, 451 (2007).
7. Clark E.L., Krushelnick K., Zepf M., Beg F.N., Tatarakis M., Machacek A., Santala M.I.K., Watts I., Norreys P.A., Dangor A.E. *Phys. Rev. Lett*., **85**, 1654 (2000).
8. Hegelich M., Karsch S., Pretzler G., Habs D., Witte K., Guenther W., Allen M., Blazevic A., Fuchs J., Gauthier J.C., Geissel M., Audebert P., Cowan T., Roth M. *Phys. Rev. Lett.*, **89**, 085002 (2002).
9. Volkov R.V., Golishnikov D.M., Gordienko V.M., Dzidzoev M.S., Lachko I.M., Mar'in B.V., Mikheev P.M., Savel'ev A.B., Uryupina D.S., Shashkov A.A. *Kvantovaya Elektron.*, **33**, 981 (2003) [*Quantum Electron*., **33**, 981 (2003)].
10. Bochkarev S.G., Golovin G.V., Uryupina D.S., Shulyapov S.A., Andriyash A.V., Bychenkov V.Yu., Savel'ev A.B. *Phys. Plasmas*, **19**, 103101 (2012).
11. Gamaly E.G., Rode A.V., Luther-Davies B., Tikhonchuk V.T. *Phys. Plasmas*, **9**, 949 (2002).
12. Kalashnikov M.P., Osvay K., Priebe G., Ehrentraut L., Steinke S., Sandner W. *AIP Conf. Proc*., **1462**, 108 (2012).
13. Paudel Y., Frenje J., Merwin A., Renard-Le Galloudec N. *J. Instrumentation*, **6**, T08004 (2011).
14. Ivanov K.A., Shulyapov S.A., Turinge A.A., Brantov A.V., Uryupina D.S., Volkov R.V., Rusakov A.V., Djilkibaev R.M., Nedorezov V.G., Bychenkov V.Yu., Savel'ev A.B. *Contrib. Plasma Phys*., **53**, 116 (2013).
15. Gibbon P. *Short Pulse Laser Interactions with Matter* (London: Imperial College Press, 2005) p. 312.
16. Kovalev V.F., Bychenkov V.Y., Tikhonchuk V.T. *Zh. Eksp. Teor. Fiz.*, **122**, 264 (2002).
17. Beg F.N., Bell A.R., Dangor A.E., Danson C.N., Fews A.P., Glinsky M.E., Hammel B.A., Lee P., Norreys P.A., Tatarakis M. *Phys. Plasmas*, **4**, 447 (1997).
18. Malka G., Miquel J.L. *Phys. Rev. Lett*., **77**, 75 (1996).
19. Volkov R.V., Gordienko V.M., Lachko I.M., Mikheev P.M., Mar'in B.V., Savel'ev A.B. *Pis'ma Zh. Eksp. Teor. Fiz*., **76**, 171 (2002).
20. Lee K., Park S.H., Cha Y.-H., Lee J.Y., Lee Y.W., Yea K.-H., Jeong Y.U. *Phys. Rev. E*, **78**, 056403 (2008).
21. Ziegler J.F., Ziegler M.D., Biersack J.P. *Nucl. Instr. Meth. Phys. Res. B*, **268**, 1818 (2010).

22. Dinger R., Rohr K., Weber H. *J. Phys. D: Appl. Phys.*, **17**, 1707 (1984).
23. Kumar Aniruddha, Sonar V.R., Das D.K., Bhatt R.B., Behere P.G., Afzal Mohd., Kumar Arun, Nilaya J.P., Biswas D. *J. Appl. Surf. Sci.*, **308**, 216 (2014).
24. Platonenko V.T. *Laser Phys.*, **2**, 852 (1992).
25. Sobel'man I.I., Vainshtein L.A., Yukov E.A. *Excitation of Atoms and Broadening of Spectral Lines* (New York: Springer, 1995; Moscow: Nauka, 1979).
26. Delone N.B., Krainov V.P. *Usp. Fiz. Nauk*, **168**, 531 (1998).
27. Burnett N.H., Corkum P.B. *J. Opt. Soc. Am. B*, **6**, 1195 (1989).
28. Volkov R.V., Gordienko V.M., Lachko I.M., Rusanov A.A., Savel'ev A.B., Uryupina D.S. *Zh. Eksp. Teor Fiz.*, **130**, 347 (2006).
29. Rusanov A.A., Savel'ev A.B. *Laser Phys.*, **14**, 1466 (2004).
30. Zel'dovich Ya.B., Raizer Yu.P. *Physics of Shock Waves and High-Temperature Hydrodynamic Phenomena* (New York: Dover Publications, 2002; Moscow: Nauka, 1966).
31. Kramida A., Ralchenko Y., Reader J. *NIST ASD Team, NIST Atomic Spectra Database* (ver. 5.2), National Institute of Standards, Technology, Gaithersburg, MD.
32. Tikhonchuk V.T. *Phys. Plasmas*, **9**, 1416 (2002).
33. Zhidkov A.G., Sasaki A., Tajima T., Auguste T., D'Olivera P., Hulin S., Monot P., Faenov A.Ya., Pikuz T.A., Skobelev I.Yu. *Phys. Rev. E*, **60**, 3273 (1999).